J. Am. Soc. Mass Spectrom. (2016) 27:1914–1921
DOI: 10.1007/s13361-016-1493-y

RESEARCH ARTICLE

Multigenerational Broadband Collision-Induced Dissociation of Precursor Ions in a Linear Quadrupole Ion Trap

Dalton T. Snyder, R. Graham Cooks

Department of Chemistry and Center for Analytical Instrumentation Development, Purdue University, West Lafayette, IN 47907, USA

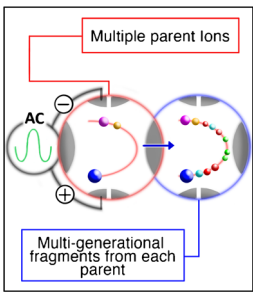

Abstract. A method of fragmenting ions over a wide range of *m*/*z* values while balancing energy deposition into the precursor ion and available product ion mass range is demonstrated. In the method, which we refer to as "multigenerational collision-induced dissociation", the radiofrequency (rf) amplitude is first increased to bring the lowest *m*/*z* of the precursor ion of interest to just below the boundary of the Mathieu stability diagram (q = 0.908). A supplementary AC signal at a fixed Mathieu q in the range 0.2–0.35 (chosen to balance precursor ion potential well depth with available product ion mass range) is then used for ion excitation as the rf amplitude is scanned downward, thus fragmenting the precursor ion population from high to low *m*/*z*. The method is shown to generate high intensities of product ions compared with other broadband CID methods while retaining low mass ions during the fragmentation step, resulting in extensive fragment ion coverage for various components of complex mixtures. Because ions are fragmented from high to low *m*/*z*, space charge effects are minimized and multiple discrete generations of product ions are produced, thereby giving rise to "multigenerational" product ion mass spectra.

Keywords: Linear ion trap, Broadband fragmentation, Stored waveform inverse Fourier transform, Multigenerational CID

Received: 6 June 2016/Revised: 29 July 2016/Accepted: 1 August 2016/Published Online: 19 September 2016

Introduction

This paper is the second in a series of three that demonstrate the expanding capabilities of quadrupole ion traps for tandem mass spectrometry (MS/MS). In a first method, ion isolation is addressed with a dual frequency isolation technique [1]. The third paper deals exclusively with resolution improvements in mass spectra recorded using resonance ejection and secular frequency scanning by means of a dual frequency ejection waveform [2]. This paper concerns itself with the intermediate step in MS/MS, the dissociation of precursor ions into product ions.

Collision-induced dissociation (CID) of ions in quadrupole ion traps lends many benefits to mass spectrometry as a method of complex mixture analysis. Dissociation of isolated precursor ions into their respective fragments gives information about the structure of the precursor ion, allowing structural elucidation of unknowns. Each stage of CID also increases signal-to-noise since the inherent chemical noise is filtered out [3]. Analyte selectivity is increased via selected (or multiple) reaction monitoring (SRM/MRM), which is particularly useful for quantitative analysis [4, 5].

The primary method of CID in ion traps is resonance excitation [6, 7], wherein a small AC signal is applied in a dipolar manner to opposite trap electrodes, thereby generating an additional oscillating field to supplement the quadrupole field provided by the driving radio frequency (rf) waveform. If the frequency of this signal matches the secular frequency ($\omega_u = \beta_u\Omega/2$, where u is a dimension of the quadrupole field, β is the Mathieu parameter, and Ω is the angular rf frequency) of ions of a given *m*/*z*, then these ions will be excited to larger trajectories within the trap. As they gain kinetic energy from the rf field and collide with intentionally-introduced bath gas molecules, they will fragment because of conversion of kinetic energy to internal energy [8, 9].

There are various ways in which ions having a small range of *m*/*z* values may be fragmented. Among them are red-shifted off-resonance large-amplitude excitation (RSORLAE) [10], high amplitude short time excitation (HASTE) [11], and the similar "fast excitation" CID [12], dynamic collision-induced dissociation (DCID) with fundamental and higher-order excitation frequencies [13–15], and off-resonance CID using beat frequencies [16].

Correspondence to: R. G. Cooks; *e-mail:* cooks@purdue.edu

Methods of broadband excitation also exist. Note that there are several reasonable definitions of "broadband." When discussing *broadband waveforms*, broadband refers to the combination of multiple frequencies. Here we refer to *broadband CID* as a process in which a large range of *m/z* values is excited, either simultaneously or in a single step (as in a single ramp of the rf amplitude). In this paper, the latter definition of broadband is used exclusively.

A secular frequency scan [17–20] can be used to fragment ions of different mass/charge ratios as a function of time (broadband CID) by sweeping the frequency of the supplementary AC at constant rf amplitude. However, the method is limited by the different q values at which each ion fragments; this restricts energy deposition into some precursor ions and limits product ion mass range for others.

A second method of broadband dissociation is dipolar DC collisional activation, in which DC potentials of opposite polarities are applied to opposite electrodes, thus displacing the ion cloud from the center of the trap [21, 22]. The ions absorb power via slow rf heating and eventually dissociate. Dipolar DC CID is simpler than other methods since only a DC potential is needed, and multiple generations of product ions can be observed, but only a few analytes have been studied and there is very limited *m/z* selectivity because ion secular frequencies are not interrogated.

Another method for simultaneous excitation or ejection of multiple ions is the stored waveform inverse Fourier transform (SWIFT) [23–25], although it is generally used to perform ion isolation rather than to dissociate a set of ions. The masses of the ions to be excited or ejected are converted to secular frequencies for incorporation into a complex waveform consisting of sinusoids spaced every ~100–500 Hz with phases calculated according to a quadratic function so that the power is distributed evenly throughout [26]. The waveform is then applied for a short time in a dipolar manner, resulting in broadband excitation of ions.

Here we introduce a method of broadband dissociation, "multigenerational CID," in which a reverse rf amplitude ramp is combined with a fixed frequency resonance excitation waveform. With this method, which is most similar to Wideband Activation™ [27], ions over a broad *m/z* range are fragmented, all at the same Mathieu q value, which is chosen to balance mass range and product ion intensity. Product ion mass range is increased by fragmenting at low Mathieu q while the deposition of sufficient energy into the precursor ion to effect fragmentation is improved by placing the ion at a high Mathieu q to increase its potential well depth. The name of the method is derived from the fact that, as we will show, multiple generations of product ions can be produced as the result of more than one discrete stage of CID, thereby giving "multigenerational" product ion mass spectra that are reminiscent of high-energy CID.

Experimental

Ionization

Nanoelectrospray ionization at ~2–3 kV was used for ion production. Borosilicate glass capillaries (1.5 mm o.d., 0.86 mm i.d., Sutter Instrument Co.) were pulled to an approximate o.d. of 5 μm using a Flaming/Brown micropipette puller, also from Sutter Instrument Co. (model P-97; Novato, CA, USA).

Chemicals

p-Bromoaniline was purchased from Eastman Kodak Co. (Rochester, NY, USA). 2,4-Dichloroaniline and 4-chloroaniline were purchased from Aldrich Chemical Company, Inc. (Milwaukee, WI, USA). Tetraheptylammonium chloride was purchased from Fluka (Buchs, Switzerland), tetrabutylammonium iodide was obtained from Fluka, hexadecyltrimethylammonium bromide was obtained from Sigma (St. Louis, MO, USA), tetrahexylammonium bromide was obtained from Fluka, and tetraoctylammonium bromide was purchased from Aldrich. Reserpine was obtained from Sigma. Reagents were dissolved in 50:50 methanol:water with 0.1% formic acid to obtain final concentrations of ~5–100 ppm.

Instrumentation

All experiments were performed in the positive ion mode using the Mini 12 miniature mass spectrometer developed in-house at Purdue University [28, 29]. The Mini 12 uses a rectilinear ion trap (RIT) [30] with inner radii 4.0 mm in y and 5.0 mm in x (i.e., a stretched geometry). Ion introduction and vacuum conditions were controlled with a discontinuous atmospheric pressure interface (DAPI) [31] as well as miniature turbo and diaphragm pumps.

The general scan function for multigenerational CID as well as its illustration on the well-known Mathieu stability diagram are shown in Figure 1. Ions were injected into the RIT through a discontinuous atmospheric pressure interface (DAPI) that was open for ~13 ms. The ion population was then allowed to collisionally cool to the center of the trap for ~600 ms as the pressure inside the vacuum chamber dropped to <1 mTorr. At the end of the cooling step the rf amplitude was raised to isolate the range of precursor ions of interest. The cooling step was followed by a 200 ms CID stage in which either (1) a single AC frequency (either 80 or 100 kHz, q_x = 0.22 or q_x = 0.28, respectively) of decreasing amplitude was applied in a dipolar manner to the trap during a reverse rf amplitude ramp, or (2) a SWIFT waveform consisting of a broad range of frequencies 10–500 kHz was applied to effect broadband dissociation while the rf amplitude was kept constant at an appropriate value. The CID stage was then followed by a ~270 ms cooling period to allow the resulting product ions to decrease their amplitudes in the trap and a 300 ms resonance ejection mass scan at 349 kHz (rf frequency = 0.999 MHz) in order to record a mass spectrum from *m/z* 100 to 800. All scans shown are the average of three single scans.

Note that the 270 ms collisional cooling period is long relative to that used in a benchtop instrument (in which a cooling period would be on the order of 10 ms) because of the Mini 12's vacuum system. When the DAPI valve closes, the pressure in the vacuum manifold decreases to ~1 mTorr in

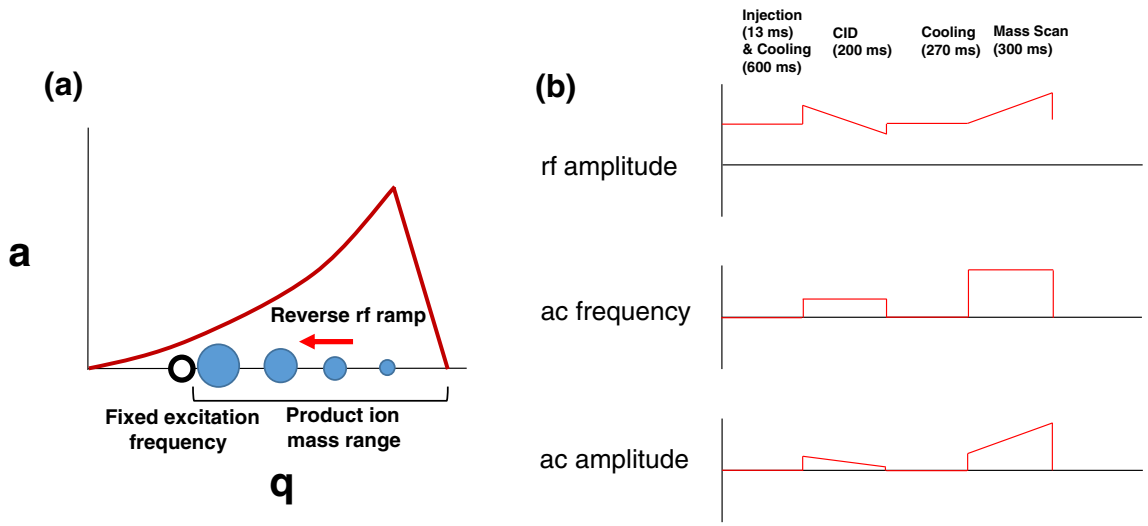

Figure 1. Multigenerational collision-induced dissociation for broadband CID in an ion trap. The method is illustrated (**a**) on the Mathieu stability diagram, where ions are fragmented in order of decreasing *m/z* by fixing the frequency of a supplementary excitation signal at an optimal q (generally in the range 0.20–0.35) just below the lowest q value (above the highest *m/z*) of interest and ramping the rf amplitude downwards. The scan table (**b**) shows the amplitude of the rf and AC and the frequency of the AC as a function of time. Note that during the alternative SWIFT excitation method, the rf amplitude during CID was constant.

~500 ms, at which point a resonance ejection scan would normally take place. However, because the ions are first collisionally cooled after the DAPI opening and then subjected to a relatively long CID step, the pressure in the trap falls to ca. 10^{-5} Torr during the second collisional cooling step, which explains why so long a cooling period is needed. A benchtop instrument in which the pressure in the ion trap is carefully regulated should not need so long a cooling period.

In this paper, we differentiate between two different low-mass cutoffs (LMCO). The *precursor ion* LMCO (the lowest *m/z* precursor ion that will be stored during the CID step) is determined by the rf amplitude at the start of the CID step (Figure 1b, rf amplitude). The second kind of LMCO is the *product ion* LMCO, which corresponds to the lowest *m/z* product ion that can be detected during the mass scan. The product ion LMCO is determined either by the lowest rf amplitude at the end of the CID step, or by the rf amplitude during the subsequent cooling step.

Results and Discussion

In general, there are two methods of performing broadband CID, that is, of fragmenting ions covering a wide *m/z* range. Ions can either be fragmented at (1) constant Mathieu q parameter, or (2) variable Mathieu q parameter. An example of the latter method is SWIFT excitation. Methods that fragment ions at different Mathieu q optimally excite a small portion of the ions but could also eject others because of their lower pseudopotential well depths (which is a function of both Mathieu q and rf amplitude) [32]. Furthermore, the available mass range for each precursor ion will be different. Precursors at high q will generate product ions that will immediately be ejected from the trap, whereas precursor ions at very low q will be ejected during excitation. It is for this reason that CID is usually performed at a q value that balances the product ion mass range against the energy deposition into the precursor ion. The result is a choice of Mathieu q of 0.2–0.35 in most cases.

This balance in ion trap CID conditions motivated us to develop a method that has two characteristics: (1) precursor ions over a large *m/z* range should fragment to give high product ion intensities, and (2) each precursor ion subject to CID should have the same fractional product ion mass range. These characteristics are obtained simply by setting the excitation waveform at a constant frequency (see AC frequency, Figure 1b). On the Mathieu stability diagram (Figure 1a), the excitation is illustrated by a stationary "hole" on the q axis. In order to fragment a broad range of ions, the rf amplitude must then be scanned. Although there are many benefits to scanning the rf in the forward direction [33, 34], including higher sensitivity and better resolution, these are limited to the *mass scan*. For the purpose of broadband CID, it is more beneficial to sweep the rf amplitude in the *reverse* direction. First, all precursor ions that are subject to CID have the same fractional product ion mass range, and the fragment ions are preserved since their q values decrease during the fragmentation step, which is similar to pulsed q dissociation and similar methods [11, 12, 35]. A second reason for scanning the rf amplitude in the reverse direction is that ion secular frequencies will shift away from the working point [33, 36–39] (assuming a positive octopole contribution) as the rf is being scanned, thereby giving each ion longer to be at or near resonance. This is particularly important during a scan in which each ion is only excited for a short period of time, unlike SWIFT. Yet a third reason is that space charge effects are minimized by first exciting those that

lie on the outside of the ion cloud, viz. the high mass ions, rather than attempting to 'peel the onion from the inside' by first exciting low mass ions [40].

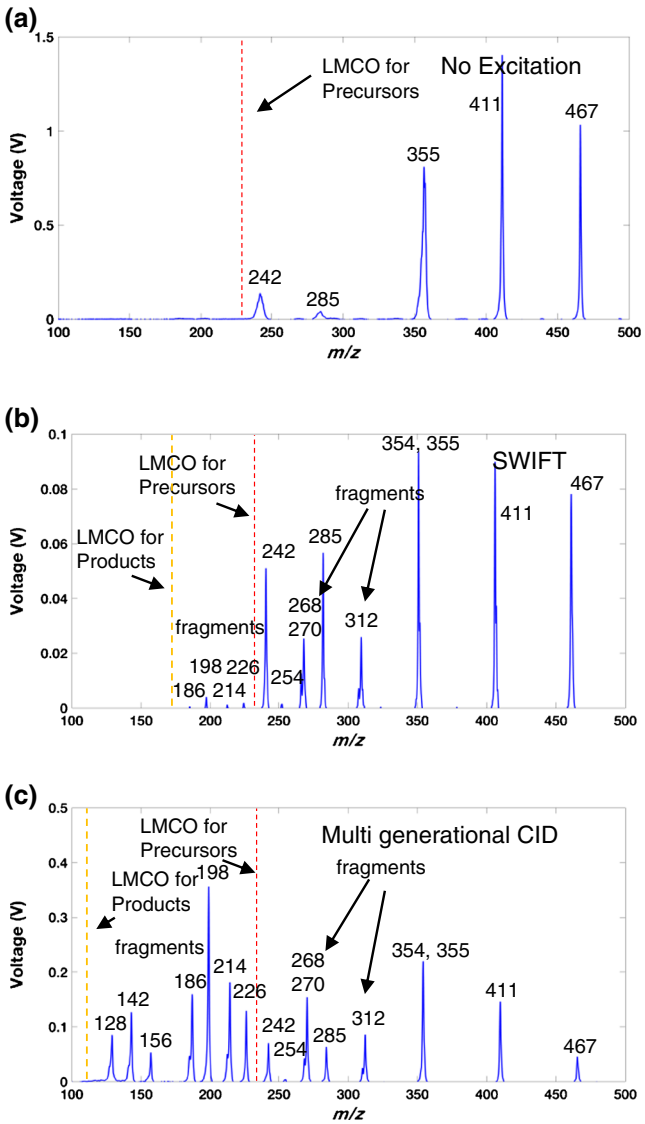

Figure 2. Comparison of multigenerational CID to SWIFT excitation and dissociation: (**a**) "blank" excitation spectrum obtained with the scan function in Figure 1b with an AC amplitude of 0 V_{pp}, showing the precursor ions and the precursor ion LMCO (dotted red line) imposed during the CID step; (**b**) SWIFT excitation spectrum with CID over 210 ms at the (constant) optimized rf amplitude of 372 $V_{0\text{-}p}$; (**c**) multigenerational CID spectrum obtained with a constant AC frequency of 80 kHz and ramped amplitude from 2.95 to 0.93 $V_{p\text{-}p}$ during a 200 ms rf amplitude ramp from 464 to 127 $V_{0\text{-}p}$. Each CID step was followed by 270 ms of cooling and a 300 ms resonance ejection scan during which the rf amplitude was ramped from 188 to 1536 $V_{0\text{-}p}$ at an AC frequency and amplitude of 349 kHz, 6.1 $V_{p\text{-}p}$. Analytes were five quaternary amines: tetrabutylammonium (*m/z* 242), hexadecyltrimethylammonium (*m/z* 284), tetrahexylammonium (*m/z* 355), tetraheptylammonium (*m/z* 411), and tetraoctylammonium (*m/z* 467). See Table 1 for relationship between parent and product ions.

A second important parameter during the CID scan is the AC amplitude, which should be ramped from high to low to accommodate the fact that ions are excited from high mass to low mass. This accomplishes two things: (1) it scales the excitation to the potential well depth of each ion so that ions of each mass are given an appropriate amount of energy (not too much, not too little), and (2) it prevents product ions from being ejected from the trap after they are produced. As we will show later, due to the choice of scan direction, multiple generations of product ions are observed in a single scan, giving rise to product ion distributions unlike that of single stage MS/MS.

In the experiments performed here, the scan function in Figure 1b was used. After the CID scan just described, ions were allowed to cool for ~270 ms, after which they were ramped out in typical resonance ejection fashion by increasing the amplitude of both the rf and AC while keeping both frequencies the same (999 and 349 kHz, respectively). As noted previously, the second collisional cooling step is long due to the low pressure ($<10^{-5}$ Torr) in the trap at times near the end of the scan table.

The full scan resonance ejection mass spectrum of five quaternary amines (tetraheptylammonium, *m/z* 411; tetrabutylammonium, *m/z* 242; hexadecyltrimethylammonium, *m/z* 285; tetrahexylammonium, *m/z* 355; and tetraoctylammonium, *m/z* 467, all molecular cations) obtained on the Mini 12 mass spectrometer is shown in Figure 2a. The spectrum can be considered a "blank excitation" since the scan function in Figure 1b was used, but without application of the supplemental AC signal during the CID step. The high starting rf amplitude during the CID step imposes a relatively high low-mass cutoff for the precursor ions that is indicated by the red dotted lines. Any product ions having a mass/charge ratio less than that corresponding to this precursor ion LMCO will not be stored unless the rf amplitude is lowered before or during CID. Fortunately, we are ramping the rf amplitude in the *reverse* direction, and as a result the LMCO for product ions is continually decreasing, allowing them to be stored in the trap as they are produced.

Figure 2b shows the result of applying a 210 ms SWIFT waveform for ion excitation followed by 200 ms cooling and an ion scan out step. In terms of the scan table in Figure 1b, the precursor ions were still isolated just before CID by quickly increasing the rf amplitude so that *m/z* 242 was the lowest *m/z* precursor ion stored. Then, instead of ramping the rf amplitude, as in Figure 1b, the rf amplitude at the beginning of the SWIFT

Table 1. Precursor Ions and Their Respective Product ions in Figure 2*. Note that many more product ions are observed with multi-stage CID, and the product ion intensities are higher.

Precursor *m/z*	Product *m/z*
242	142^{M}, $186^{S,M}$
285	200, $268^{S,M}$
355	128^{M}, $186^{S,M}$, $198^{S,M}$, $270^{S,M}$
411	142^{M}, $214^{S,M}$, $226^{S,M}$, $312^{S,M}$
467	156^{M}, $242^{S,M}$, $254^{S,M}$, $354^{S,M}$

* Data obtained using an LTQ XL linear ion trap.
M = observed with multigenerational CID.
S = observed with SWIFT.

CID step was adjusted to a fixed, lower, and optimal value that gave the best distribution and intensities of product ions. Note that this then lowered the product ion LMCO compared with the precursor ion LMCO. Because the rf amplitude was constant, the product ion LMCO did not change during the CID rf scan. Product ions *m/z* 268, 270, and 312 were observed, but the *product ion* LMCO at ~*m/z* 175 imposed by the fixed and relatively high rf amplitude during the excitation step prevents fragments with *m/z* <175 from being observed. That is, because the rf amplitude is adjusted just before excitation to optimally fragment the precursor ions, a relatively high LMCO for the product ions is enforced. Note that the experiments in which the rf amplitude was ramped from high to low during SWIFT excitation returned poor results and therefore are not shown. The SWIFT amplitude and time of application were also optimized, but the varying q values of the precursor ions prevent broad product ion coverage.

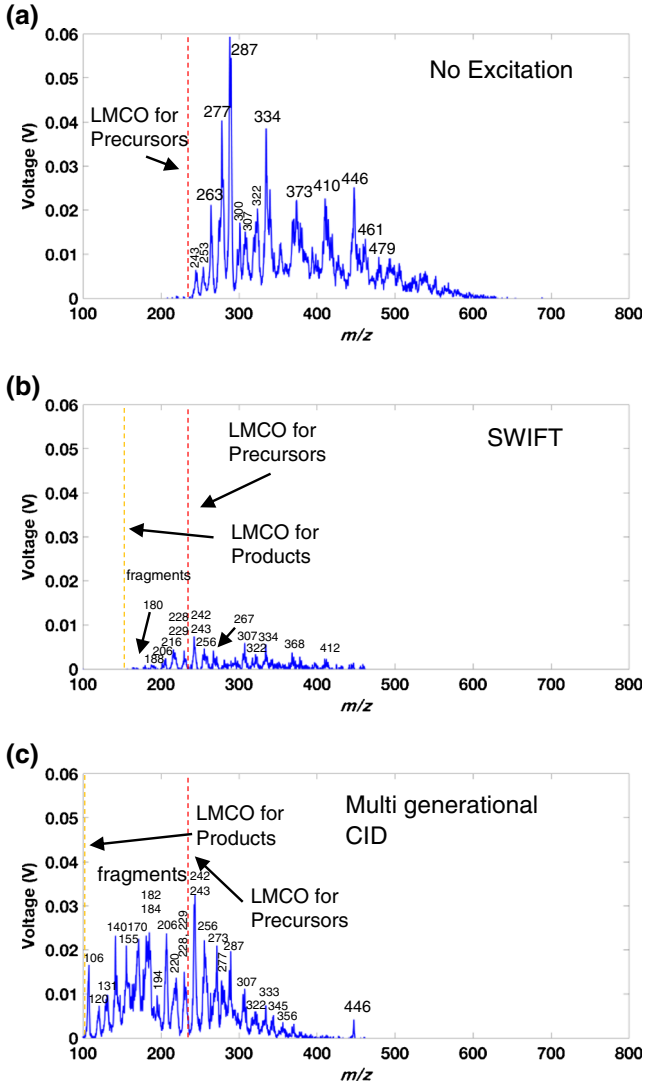

Figure 3. Comparison of multigenerational CID to SWIFT CID: (**a**) "blank" excitation spectrum obtained with the scan function in Figure 1b with an AC amplitude of 0 $V_{p\text{-}p}$, showing the precursor ions and the precursor ion LMCO (dotted red line) imposed during the CID step; (**b**) SWIFT excitation spectrum with CID over 210 ms at the (constant) optimized rf amplitude of 249 $V_{0\text{-}p}$. (**c**) Multigenerational CID spectrum with a constant AC frequency of 100 kHz and ramped amplitude from 2.08 to 1.07 $V_{p\text{-}p}$ during a 200 ms rf amplitude ramp from 525 to 127 $V_{0\text{-}p}$. Each CID step was followed by 270 ms of cooling and a 300 ms resonance ejection scan where the rf amplitude was ramped from 188 to 1536 $V_{0\text{-}p}$ with an AC frequency and amplitude of 349 kHz, 6.1 $V_{p\text{-}p}$. Analytes were 2,4-dichloroaniline, chloroaniline, and p-bromoaniline, along with any impurities, reaction products, and metabolites therein. See Table 2 for precursor ions and their corresponding product ions.

Figure 2c provides a stark contrast to the SWIFT excitation data. To obtain Figure 2c, a multigenerational CID method was used (Figure 1b, AC frequency 80 kHz, $q_x = 0.22$). Fragment ion coverage is better because the rf amplitude is ramped from high to low, retaining *m/z* 128, 142, and 156 in the trap, and product ion intensity is quite high compared with SWIFT due to the correct scaling of AC amplitude with respect to *m/z*, despite the short excitation period for each ion. The relationships between precursor ions and product ions, obtained on an LTQ XL, Thermo Fisher, San Jose, CA, USA, are shown in Table 1 for comparison. In addition, Table 1 indicates which ions were observed with SWIFT excitation and which were observed with multigenerational CID.

Figure 3a shows the full scan "blank excitation" of a second mixture, which is more complex. The intentionally introduced analytes were halogenated anilines, viz. chloroaniline, 2,4-dichloroaniline, and 4-bromoaniline. However, as shown, the actual mixture is considerably more complex with many peaks being observed. The precursor ion LMCO imposed during the blank CID step was chosen so that the signals attributable to the three introduced analytes were removed, thereby leaving only signals due to impurities and metabolites above ~*m/z* 220. Here we performed broadband CID to demonstrate the acquisition of

Table 2. Precursor Ions and Their Respective Product Ions in Figure 3*. Note that many more product ions are observed with multigenerational CID, and the product ion intensities are higher.

Precursor *m/z*	Product *m/z*
243	208, 106^{M}
253	222, $218^{S,M}$, 194^{M}, 182^{M}, 150^{M}, 120^{M}, 106^{M}
263	248, 235, $228^{S,M}$, $220^{S,M}$, 213
277	$242^{S,M}$, $206^{S,M}$, 140^{M}, 106^{M}
287	$256^{S,M}$, $207^{S,M}$, 184^{M}, 120^{M}, 106^{M}
297	$265^{S,M}$, 247, $205^{S,M}$, 128
300	$273^{S,M}$, 234, 197
307	292^{M}, 279, 275, $240^{S,M}$, $228^{S,M}$, 213, 196, 170^{M}
322	$307^{S,M}$, 294, $286^{S,M}$, $243^{S,M}$, 184^{M}, 140^{M}
334	$307^{S,M}$, 298, 231, 197
339	$324^{S,M}$, 311, $307^{S,M}$, 304, 289^{M}, 246, 236, 213, $188^{S,M}$
352	337, $324^{S,M}$, $320^{S,M}$, 249, 215^{S}
368	352, 341, $333^{S,M}$, $287^{S,M}$, $229^{S,M}$, 212, $186^{S,M}$
373	358, $345^{S,M}$, 341, 338, 313, 280, 246, 222, $186^{S,M}$
410	393, 382, 375, $333^{S,M}$, $307^{S,M}$, $299^{S,M}$, $273^{S,M}$
446	431, 418, 353^{M}, 343^{M}, 335, $319^{S,M}$, $309^{S,M}$, $307^{S,M}$, 291^{M}
461	444, 434, 425, 368, 358, $334^{S,M}$, $324^{S,M}$, $322^{S,M}$

*Data obtained using an LTQ XL linear ion trap.
M = observed with multigenerational CID.
S = observed with SWIFT.

a significant portion of MS^n space. The SWIFT excitation spectrum is shown in Figure 3b, and it suffers from the constraint of a constant product ion LMCO, which is the direct result of increasing the rf amplitude during the CID step. The spectrum in Figure 3c, however, does not exhibit such a high product ion LMCO because the rf amplitude is ramped from high to low with a constant frequency and decreasing excitation amplitude. Once again, product ion coverage is better when multigenerational CID is used, although the limited resolution of the Mini 12 prevents many product ions from being resolved. See Table 2 for precursor and product ions obtained via CID on an LTQ XL. In particular, we notice that multigenerational CID is particularly useful for retaining low mass product ions.

The most interesting consequence of scanning the rf amplitude in the reverse direction and thus fragmenting from high to low *m/z* is that multiple generations of fragment ions may be observed. That is, because ions are fragmenting successively from high to low mass, a precursor ion will fragment early in the CID rf scan and generate first generation product ions. These product ions can then dissociate later in the scan in a second discrete step because their secular frequencies are decreasing toward the excitation frequency as the rf amplitude is ramped. Hence, we observe more than one generation of fragments from "multigenerational CID." The product ion mass spectra that are produced will thus be combinations of fragments that are observed with discrete MS^2, MS^3, and higher order MS^n operations.

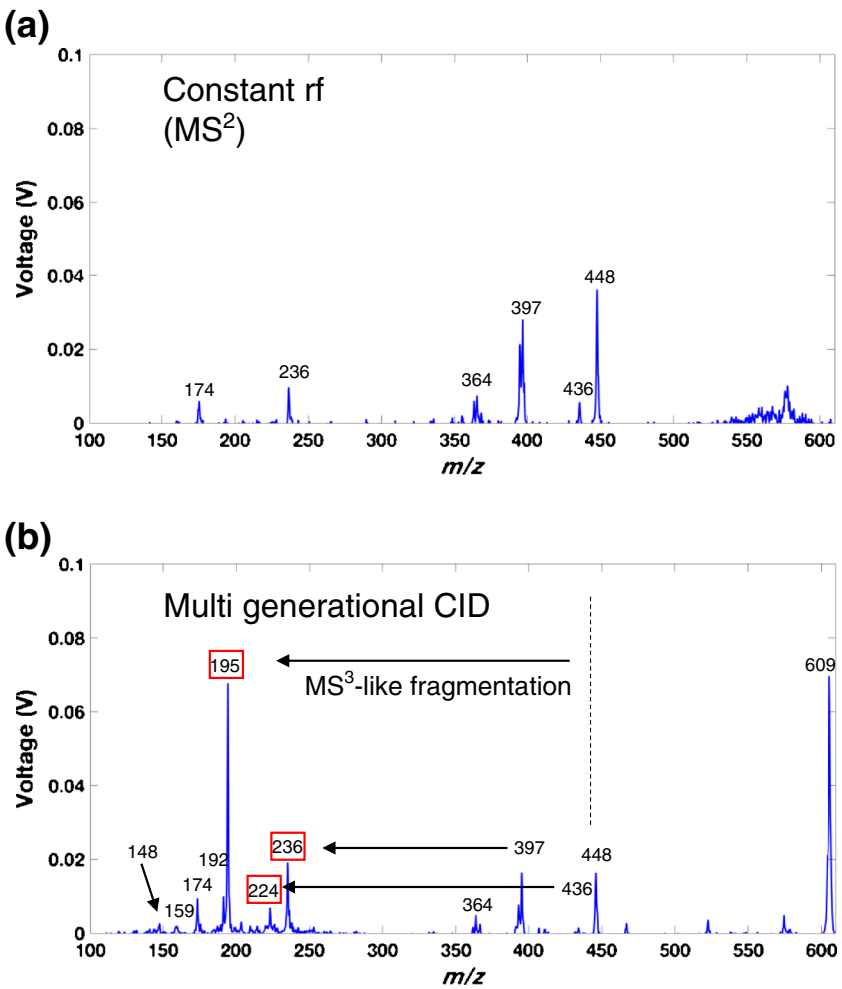

Figure 4. Observation of multiple generations of product ions in multigenerational CID: (**a**) shows the product ion MS^2 CID spectrum of reserpine (*m/z* 609; mass selected precursor ion) under constant rf amplitude conditions and resonance excitation for 50 ms at 75 kHz (q = 0.21); (**b**) shows the multigenerational CID spectrum (Figure 1b). The ions highlighted in red boxes are product ions of *m/z* 397 and 448, which indicates that multiple stages of dissociation have been performed (i.e., MS^3). For (**a**), reserpine was excited at 75 kHz, 1.5 V_{p-p}, for 50 ms with an rf amplitude of 311 V_{0-p} followed by 300 ms of cooling and a 300 ms resonance ejection scan from an rf amplitude of 188 to 1536 V_{0-p} with an AC frequency and amplitude of 349 kHz, 6.1 V_{p-p}. During the 200 ms CID stage in (**b**) the rf amplitude was ramped from 1076 to 127 V_{0-p} while the AC signal at 85 kHz (q = 0.24) was ramped from 3.95 to 1.22 V_{pp}. This was followed by a 250 ms cooling period and a 300 ms resonance ejection scan where the rf amplitude was ramped from 188 to 1536 V_{0-p} with an AC frequency and amplitude of 349 kHz, 6.1 V_{p-p}.

Figure 4 demonstrates this phenomenon for protonated reserpine (*m/z* 609, $[M + H]^+$). A typical constant rf product ion MS/MS spectrum is given in Figure 4a. The ions observed, *m/z* 174, 236, 364, 397, 436, and 448, and their relative intensities, are nearly identical to those obtained using other linear ion traps (e.g., an LTQ XL, not shown). The precursor ion is not observed because of the relatively long time it is on resonance. The multigenerational CID mass spectrum (Figure 4b) is somewhat different and resembles spectra obtained under higher energy conditions. See reference [41] for a high energy (i.e., triple quadrupole) MS/MS spectra of reserpine. Although absolute intensities between the spectra in Figure 4 should not be compared, in general, high mass product ions have lower relative intensities and lower mass ions have higher relative intensities as seen in panel b. It should also be kept in mind that the amount of time each ion is on resonance during multigenerational CID is much shorter than in conventional constant rf resonance excitation. More importantly, different ions are observed as a result of multiple stages of fragmentation. For example, product ion *m/z* 448 was observed to fragment to *m/z* 195 using an LTQ XL (in an MS^3 experiment). The intensity of this peak is quite high, indicating efficient fragmentation of both the precursor and the first generation product ion. Furthermore, *m/z* 224 was determined to be the result of fragmentation of *m/z* 436, which is observed in Figure 4a but hardly present in Figure 4b, and *m/z* 236 is the product of fragmentation of *m/z* 397. These extra signals, that is, the observation of multiple generations of product ions in multigenerational CID, are a useful source of additional information that serves to characterize the precursor ion.

Further inspection reveals that multigenerational CID expands the capabilities of single ion traps and therefore increases the utility of the ion trap. For example, current multiple reaction monitoring methods in traps require multiple ion injections, isolations, and mass scan steps. However, with multigenerational CID, only one isolation, CID, and mass scan sequence is needed, assuming each precursor ion has a unique product ion that can be used for quantitation. Furthermore, the multiple generations of fragmentation that are observed can be used to obtain product ion spectra that more closely resemble those from higher energy instruments (e.g., triple quadrupoles), possibly allowing for the differentiation of isomers and further fragmentation of molecules that otherwise give little information in MS^2. For this reason, the field of forensics and space exploration (e.g., NASA missions) may find particular interest in multigenerational CID. For such applications, either a significant backlog of samples or a limited amount of sample and limited ion injections would benefit from a method that can obtain unique mass spectra using fewer scan sequences.

Conclusion

We have introduced a method of broadband ion activation in quadrupole ion traps in which the rf amplitude is ramped downwards while a constant frequency but decreasing amplitude AC signal is used for mass selective ion excitation. The method, termed "multigenerational CID," consistently exhibits higher product ion intensities and better product ion mass ranges compared with SWIFT, despite limited activation time. Multiple discrete stages of dissociation can be observed with this technique because of the nontraditional scan direction.

This method is one of a suite of technologies recently developed that expand ion trap capabilities, simplify instrumentation, and improve performance. Other steps in CID are readily implemented using the dual frequency isolation technique and successive resonances for ion ejection.

Acknowledgments

The authors acknowledge funding from NSF (CHE 1307264) and NASA (NNX16AJ25G).

References

1. Snyder, D.T., Cooks, R.G.: Ion isolation in a linear ion trap using dual resonance frequencies. doi:10.1007/s13361-016-1494-x
2. Snyder, D.T., Cooks, R.G.: Successive resonances for ion ejection at arbitrary frequencies in an ion trap. doi:10.1007/s13361-016-1473-2
3. de Hoffman, E.: Tandem mass spectrometry, a primer. J. Mass Spectrom. **31**, 129–137 (1996)
4. Yost, R.A., Enke, C.G.: Triple quadrupole mass spectrometry for direct mixture analysis and structure elucidation. Anal. Chem. **51**, 1251–1264 (1979)
5. Kondrat, R.W., Mcclusky, G.A., Cooks, R.G.: Multiple reaction monitoring in mass spectrometry mass spectrometry for direct analysis of complex mixtures. Anal. Chem. **50**, 2017–2021 (1978)
6. Fulford, J.E., Nhu-Hoa, D., Hughes, R.J., March, R.E., Bonner, R.F., Wong, G.J.: Radio-frequency mass selective excitation and resonant ejection of ions in a three-dimensional quadrupole ion trap. J. Vac. Sci. Technol. **17**, 829–835 (1980)
7. March, R.E., McMahon, A.W., Londry, F.A., Alfred, R.L., Todd, J.F.J., Vedel, F.: Resonance excitation of ions stored in a quadrupole ion trap. Part 1. A simulation study. Int. J. Mass Spectrom. Ion Processes **95**, 119–156 (1989)
8. Goeringer, D.E., McLuckey, S.A.: Kinetics of collision-induced dissociation in the Paul trap: A first-order model. Rapid Commun. Mass Spectrom. **10**, 328–334 (1996)
9. Splendore, M., Londry, F.A., March, R.E., Morrison, R.J.S., Perrier, P., Andre, J.: A simulation study of ion kinetic energies during resonant excitation in a stretched ion trap. Int. J. Mass Spectrom. Ion Processes **156**, 11–29 (1996)
10. Qin, J., Chait, B.T.: Matrix-assisted laser desorption ion trap mass spectrometry: efficient isolation and effective fragmentation of peptide ions. Anal. Chem. **68**, 2108–2112 (1996)
11. Cunningham Jr., C., Glish, G.L., Burinsky, D.J.: High amplitude short time excitation: a method to form and detect low mass product ions in a quadrupole ion trap mass spectrometer. J. Am. Soc. Mass Spectrom. **17**, 81–84 (2006)
12. Murrell, J., Despeyroux, D., Lammert, S.A., Stephenson, J.L., Goeringer, D.E.: "Fast excitation" CID in a quadrupole ion trap mass spectrometer. J. Am. Soc. Mass Spectrom. **14**, 785–789 (2003)
13. Collin, O.L., Beier, M., Jackson, G.P.: Dynamic collision-induced dissociation of peptides in a quadrupole ion trap mass spectrometer. Anal. Chem. **79**, 5468–5473 (2007)
14. Laskay, Ü.A., Collin, O.L., Hyland, J.J., Nichol, B., Jackson, G.P., Pasilis, S.P., Duckworth D.C.: Dynamic collision-induced dissociation (DCID) in a quadrupole ion trap using a two-frequency excitation waveform: II. Effects of frequency spacing and scan rate. J. Am. Soc. Mass Spectrom. **18**, 2017–2025 (2007)
15. Laskay, U.A., Jackson, G.P.: Resonance excitation and dynamic collision-induced dissociation in quadrupole ion traps using higher-order excitation frequencies. Rapid Commun. Mass Spectrom. **22**, 2342–2348 (2008)
16. Hager, J.W.: Off-resonance excitation in a linear ion trap. J. Am. Soc. Mass Spectrom. **20**, 443–450 (2009)

17. Snyder, D.T., Pulliam, C.J., Wiley, J.S., Duncan, J., Cooks, R.G.: Experimental characterization of secular frequency scanning in ion trap mass spectrometers. J. Am. Soc. Mass Spectrom. **27**, 1243–1255 (2016)
18. Johnson, J.V., Pedder, R.E., Yost, R.A.: Ms Ms parent scans on a quadrupole ion trap mass-spectrometer by simultaneous resonant excitation of multiple ions. Int. J. Mass Spectrom. Ion Processes **106**, 197–212 (1991)
19. Snyder, D.T., Pulliam, C.J., Cooks, R.G.: Single analyzer precursor scans using an ion trap. Rapid Commun. Mass Spectrom. **30**, 800–804 (2016)
20. Welling, M., Schuessler, H.A., Thompson, R.I., Walther, H.: Ion/molecule reactions, mass spectrometry and optical spectroscopy in a linear ion trap. Int. J. Mass Spectrom. Ion Processes **172**, 95–114 (1998)
21. Prentice, B.M., McLuckey, S.A.: Dipolar DC collisional activation in a "stretched" 3-D ion trap: the effect of higher order fields on rf-heating. J. Am. Soc. Mass Spectrom. **23**, 736–744 (2012)
22. Prentice, B.M., Xu, W., Ouyang, Z., McLuckey, S.A.: DC potentials applied to an end-cap electrode of a 3-D ion trap for enhanced MS functionality. Int. J. Mass Spectrom. **306**, 114–122 (2011)
23. Guan, S., Marshall, A.G.: Stored waveform inverse Fourier transform axial excitation/ejection for quadrupole ion trap mass spectrometry. Anal. Chem. **65**, 1288–1294 (1993)
24. Guan, S., Marshall, A.G.: Stored waveform inverse Fourier transform (SWIFT) ion excitation in trapped-ion mass spectometry—theory and applications. Int. J. Mass Spectrom. Ion Processes **157/158**, 5–37 (1996)
25. Julian, R.K., Cooks, R.G.: Broad-band excitation in the quadrupole ion-trap mass-spectrometer using shaped pulses created with the inverse fourier-transform. Anal. Chem. **65**, 1827–1833 (1993)
26. Guan, S.: General phase modulation method for stored waveform inverse Fourier transform excitation for Fourier transform ion cyclotron resonance mass spectrometry. J. Chem. Phys. **91**, 775–777 (1989)
27. Lopez, L.L., Tiller, P.R., Senko, M.W., Schwartz, J.C.: Automated strategies for obtaining standardized collisionally induced dissociation spectra on a benchtop ion trap mass spectrometer. Rapid Commun. Mass Spectrom. **13**, 663–668 (1999)
28. Li, L., Chen, T.C., Ren, Y., Hendricks, P.I., Cooks, R.G., Ouyang, Z.: Mini 12, miniature mass spectrometer for clinical and other applications—introduction and characterization. Anal. Chem. **86**, 2909–2916 (2014)
29. Snyder, D.T., Pulliam, C.J., Ouyang, Z., Cooks, R.G.: Miniature and fieldable mass spectrometers: recent advances. Anal. Chem. **88**, 2–29 (2016)
30. Ouyang, Z., Wu, G., Song, Y., Li, H., Plass, W.R., Cooks, R.G.: Rectilinear ion trap: concepts, calculations, and analytical performance of a new mass analyzer. Anal. Chem. **76**, 4595–4605 (2004)
31. Gao, L., Cooks, R.G., Ouyang, Z.: Breaking the pumping speed barrier in mass spectrometry: discontinuous atmospheric pressure interface. Anal. Chem. **80**, 4026–4032 (2008)
32. Dehmelt, H.G.: Radiofrequency spectroscopy of stored ions. I: Storage. Adv. At. Mol. Phys. **3**, 53–72 (1968)
33. Williams, J.D., Cox, K.A., Cooks, R.G., Mcluckey, S.A., Hart, K.J., Goeringer, D.E.: Resonance ejection ion-trap mass-spectrometry and nonlinear field contributions—the effect of scan direction on mass resolution. Anal. Chem. **66**, 725–729 (1994)
34. Wells, J.M., Plass, W.A., Cooks, R.G.: Control of chemical mass shifts in the quadrupole ion trap through selection of resonance ejection working point and rf scan direction. Anal. Chem. **72**, 2677–2683 (2000)
35. Schwartz J.C., Syka J.E.P., Quarmby S.T.: Improving the fundamentals of MS^n on 2D linear ion traps: new ion activation and isolation techniques. The 53rd ASMS Conference on Mass Spectrometry and Allied Topic; San Antonio, TX. June 5–9. (2005)
36. Makarov, A.A.: Resonance ejection from the Paul trap: a theoretical treatment incorporating a weak octapole field. Anal. Chem. **68**, 4257–4263 (1996)
37. Wang, Y., Huang, Z., Jiang, Y., Xiong, X., Deng, Y., Fang, X., Xu,W.: The coupling effects of hexapole and octopole fields in quadrupole ion traps: a theoretical study. J. Mass Spectrom. **48**, 937–944 (2013)
38. Wang, Y., Franzen, J., Wanczek, K.P.: The nonlinear resonance ion trap. Part 2. A general theoretical analysis. Int. J. Mass Spectrom. Ion Processes. **124**, 125–144 (1993)
39. Franzen, J.: The nonlinear ion trap. Part 5. Nature of nonlinear resonances and resonant ion ejection. Int. J. Mass Spectrom. Ion Processes **130**, 15–40 (1994)
40. Tomachev, A.V., Udseth, H.R., Smith, R.D.: Radial stratification of ions as a function of mass to charge ratio in collisional cooling radio frequency multipoles used as ion guides or ion traps. Rapid Commun. Mass Spectrom. **14**, 1907–1913 (2000)
41. Hager, J.W.: A new linear ion trap mass spectrometer. Rapid Commun. Mass Spectrom. **16**, 512–526 (2002)